Dissociation of Multiply Charged Negative Ions for Hirudin (54–65), Fibrinopeptide B, and Insulin A (Oxidized)

Nigel P. Ewing and Carolyn J. Cassady
Department of Chemistry and Biochemistry, Miami University, Oxford, Ohio, USA

Collision-induced dissociation (CID) was performed on multiply deprotonated ions from three commercial peptides: hirudin (54–65), fibrinopeptide B, and oxidized insulin chain A. Ions were produced by electrospray ionization in a Fourier transform ion cyclotron resonance mass spectrometer. Each of these peptides contains multiple acidic residues, which makes them very difficult to ionize in the positive mode. However, the peptides deprotonate readily making negative ion studies a viable alternative. The CID spectra indicated that the likely deprotonation sites are acidic residues (aspartic, glutamic, and cysteic acids) and the C-terminus. The spectra are rife with c, y, and internal ions, although some a, b, x, and z ions form. Many of the fragment ions were formed from cleavage adjacent to acidic residues, both N- and C-terminal to the acidic site. In addition, neutral loss (e.g., NH_3, CH_3, H_2O, and CO_2) was prevalent from both the parent ions and from fragment ions. These neutral eliminations were often indicative of specific amino acid residues. The fragmentation patterns from several charge states of the parent ions, when combined, provide significant primary sequence information. These results suggest that negative mode CID of multiply deprotonated ions provides useful structural information and can be worthwhile for highly acidic peptides that do not form positive ions in abundance. (J Am Soc Mass Spectrom 2000, 12, 105–116) © 2000 American Society for Mass Spectrometry

Since its genesis in the 1980s, electrospray ionization (ESI) [1, 2] has developed into a routine technique for the analysis of a wide variety of organic, bio-organic, and inorganic compounds. The majority of these studies have involved positive ions that are generated by proton addition to basic sites. However, many biologically significant proteins and peptides contain several acidic residues (e.g., glutamic and aspartic acids) or post-translational modifications to produce acidic groups (e.g., phosphates or sulfonates). Such peptides can be difficult to analyze by mass spectrometry in the positive ion mode [3, 4]. For these compounds, the negative ion mode, which relies on sites of deprotonation, may yield a stronger ion signal.

Over the past decade, the dissociation of protonated protein and peptide ions has been the subject of hundreds of investigations that have yielded sequence and conformational information [5–10]. In contrast, relatively little work has focused on the fragmentation of negatively charged peptide ions. In studies on tri- and tetrapeptides ionized by fast atom bombardment (FAB), it was reported that small peptide negative ions produce fewer fragments than positive ions. However, the two modes of dissociation often yield complementary

structural information [11–16]. Recent investigations in our laboratory [17–19] employing matrix-assisted laser desorption ionization (MALDI) post-source decay (PSD) [20–22] time-of-flight (TOF) mass spectrometry have shown that positive and negative ion PSD provide complementary information on peptide primary structures. In fact, for several peptides containing acidic residues, more sequence information was obtained in the negative ion mode than in the positive mode [17].

Bowie [13–16, 23–25], Beauchamp [26], and their co-workers have investigated the collision-induced dissociation (CID) of small singly charged deprotonated peptides. They found that cleavage at acidic residues is prevalent [23]. In addition, loss of small neutrals such as CO_2, NH_3, H_2O, and CH_3 from fragments is common. Only a handful of studies have dealt with the dissociation of multiply charged negative peptide and protein ions. Loo et al. [4] reported the facile generation of such ions using solutions with ammonium hydroxide added to yield a pH of ~11. In the same study, CID results were presented for $[M - 3H]^{3-}$ and $[M - 4H]^{4-}$ of oxidized insulin chain A, as studied in a triple quadrupole mass spectrometer. The spectra revealed several doubly and triply charged b and y ions including significant loss of SO_3 (80 Da). Loss of SO_3 was also reported by Gibson and co-workers [27, 28]. Summerfield and Gaskell [29] studied the decomposition of $[M - 2H]^{2-}$ for three small peptides containing cysteic

Address reprint requests to Dr. Carolyn J. Cassady, Department of Chemistry, Box 870336, The University of Alabama, Tuscaloosa, AL 35487-0336. E-mail: cassadcj@ua.edu

Hirudin (54-65), [M-3H]³⁻ and [M-2H]²⁻

$$\overset{1\quad\ 5\qquad\ 10\ 12}{\underset{12\ 10\qquad 5\qquad 1}{\text{GDFEEIPEEYLQ}}}$$

Fibrinopeptide B, [M-4H]⁴⁻ and [M-3H]³⁻

$$\overset{1\qquad\ 5\qquad\ 10\qquad 14}{\underset{14\qquad 10\qquad\ 5\qquad 1}{\text{pEGVNDNEEGFFSAR}}}$$

Insulin Chain A oxidized, [M-5H]⁵⁻ and [M-4H]⁴⁻

$$\overset{1\quad\ \ 5\qquad\quad 10\qquad\quad 15\qquad\quad 20\ 21}{\underset{21\ 20\qquad\quad 15\qquad\quad 10\qquad\quad 5\qquad\quad 1}{\text{GIVEQCyxCyxASVCyxSLYQLENYCyxN}}}$$

Figure 1. Amino acid sequences for fibrinopeptide B, hirudin (54–65), and insulin chain A oxidized. Potential deprotonation sites are in boldface.
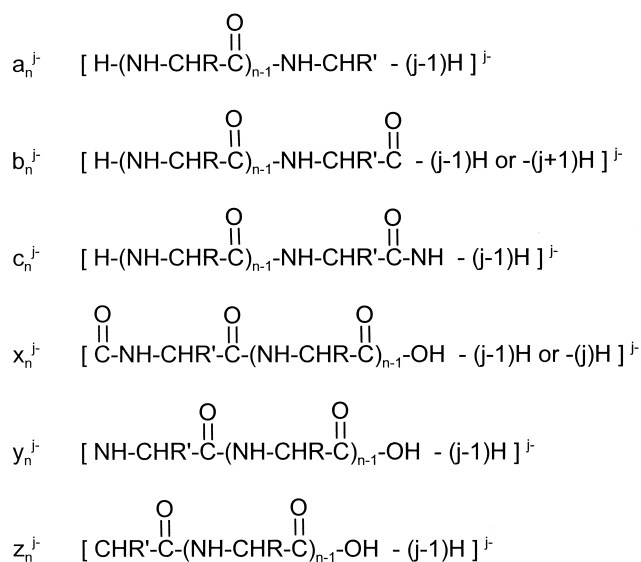
acid. They found that sequestration of the charge on this highly acidic residue was detrimental to dissociation.

In the present study, we use three commercial peptides to explore the viability of obtaining sequence information from low-energy CID on multiply charged negative ions. The multiply deprotonated ions, $[M - nH]^{n-}$, of hirudin (54–65) ($n = 2$ and 3), insulin chain A (oxidized) ($n = 4$ and 5), and fibrinopeptide B ($n = 3$ and 4) were studied in a Fourier transform ion cyclotron resonance (FT-ICR) mass spectrometer. Unfortunately, attempts to generate multiply charged positive ions for all three highly acidic peptides were futile. Figure 1 shows the one letter amino acid sequence codes for the three peptides with potential deprotonation sites given in boldface. Each of these peptides contain multiple acidic residues; thus, it is not surprising that they produce very little or no multiply charged ions in the positive mode, but generate abundant multiply charged negative ions.

Experimental

All experiments were performed using a Bruker (Billerica, MA) BioApex 47e FT-ICR mass spectrometer with a 4.7 tesla superconducting magnet [30]. Details on the instrument configuration have been previously reported [31]. Ions were generated by an Analytica of Branford (Branford, CT) electrospray source employing pneumatic-assist ESI [32, 33].

For CID experiments with sustained off-resonance irradiation (SORI) [34], ions were activated 500–1200 Hz off resonance (either higher or lower frequency) with a pulsed voltage of 6.0–18.9 V_{p-p} for times of 100–150 ms. The collision gas was xenon, which reached a maximum pressure of 10^{-5} torr. For experiments with on-resonance CID [35], ions were activated with voltages ranging from 195 to 300 V_{p-p} for times of up to 15 μs.

$$a_n^{j-}\quad [\ \text{H-(NH-CHR-}\overset{\overset{\text{O}}{\|}}{\text{C}}\text{)}_{n-1}\text{-NH-CHR'}\ \text{- (j-1)H}\ ]^{j-}$$

$$b_n^{j-}\quad [\ \text{H-(NH-CHR-}\overset{\overset{\text{O}}{\|}}{\text{C}}\text{)}_{n-1}\text{-NH-CHR'-}\overset{\overset{\text{O}}{\|}}{\text{C}}\ \text{- (j-1)H or -(j+1)H}\ ]^{j-}$$

$$c_n^{j-}\quad [\ \text{H-(NH-CHR-}\overset{\overset{\text{O}}{\|}}{\text{C}}\text{)}_{n-1}\text{-NH-CHR'-}\overset{\overset{\text{O}}{\|}}{\text{C}}\text{-NH}\ \text{- (j-1)H}\ ]^{j-}$$

$$x_n^{j-}\quad [\ \overset{\overset{\text{O}}{\|}}{\text{C}}\text{-NH-CHR'-}\overset{\overset{\text{O}}{\|}}{\text{C}}\text{-(NH-CHR-}\overset{\overset{\text{O}}{\|}}{\text{C}}\text{)}_{n-1}\text{-OH}\ \text{- (j-1)H or -(j)H}\ ]^{j-}$$

$$y_n^{j-}\quad [\ \text{NH-CHR'-}\overset{\overset{\text{O}}{\|}}{\text{C}}\text{-(NH-CHR-}\overset{\overset{\text{O}}{\|}}{\text{C}}\text{)}_{n-1}\text{-OH}\ \text{- (j-1)H}\ ]^{j-}$$

$$z_n^{j-}\quad [\ \text{CHR'-}\overset{\overset{\text{O}}{\|}}{\text{C}}\text{-(NH-CHR-}\overset{\overset{\text{O}}{\|}}{\text{C}}\text{)}_{n-1}\text{-OH}\ \text{- (j-1)H}\ ]^{j-}$$

**Figure 2.** Nomenclature and structure of dissociation fragments for multiply charged negative peptide ions.

All peptides were purchased from Sigma Chemical (St. Louis, MO) and were used without further purification. Solutions ranging in concentration from (1.6 to 2.7) × 10^{-5} M were formed in 50:50:1 mixture of methanol : water : ammonium hydroxide that had a pH of 9–11. The solution was introduced into the electrospray source at a flow rate of 5–10 μL/min and was sprayed across a +3 kV potential through a 225 °C N_2 countercurrent drying gas at >60 lb/in.² The pneumatic-assist gas was N_2 at 20 lb/in.²

Results and Discussion

Negative Ion CID Nomenclature

Figure 2 is a schematic of the nomenclature employed in the present work to describe the negative ion fragments. It is based on the positive ion nomenclature of Roepstorff and Fohlman [36]. The a, b, and c ions incorporate the N-terminus, while the x, y, and z series contain the C-terminus. The subscript n corresponds to the number of the amino acid residue (from the N-terminus) and R denotes the corresponding side chain. The charge on the fragment is denoted by $j-$. The number of hydrogens lost is also indicated in the structures. The high resolution capability of the FT-ICR facilitates determination of the number of hydrogens lost for multiply charged ions. However, because of the complexity of the spectra presented here, more research on smaller synthetic peptides is required to clearly assign sites of deprotonation and to ascertain mechanisms.

Our FT-ICR data from multiply charged ions indicate that a-, c-, y-, and z-ion series have a hydrogen differential of $-(j - 1)$, or $-j + 1$, relative to the hypothetically neutral cleaved fragment. Thus, singly charged members of these series ($j = 1$) have no added
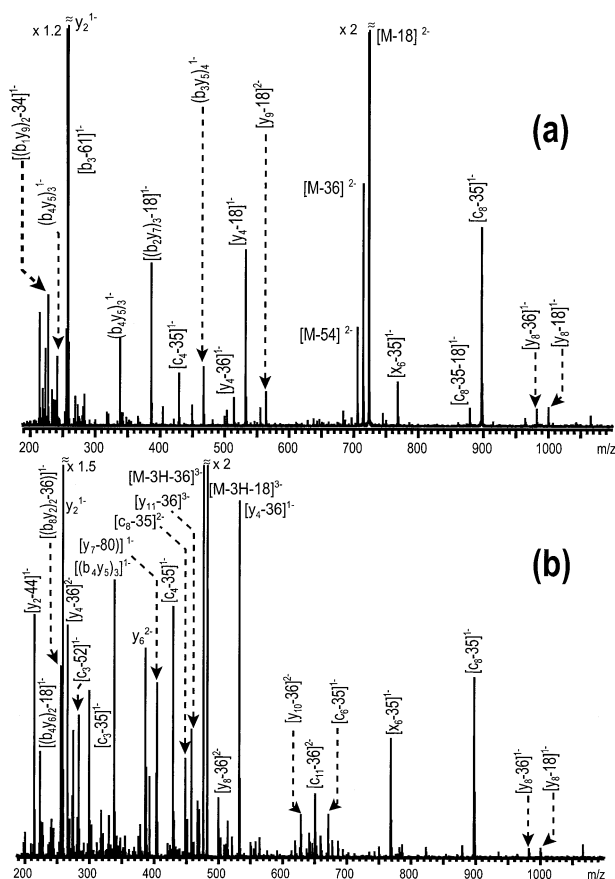
Figure 3. SORI-CID mass spectra of (**a**) $[M - 2H]^{2-}$ and (**b**) $[M - 3H]^{3-}$ for hirudin (54–65).

spectra. These assignments of $-(j - 1)$ differential hydrogens agree with PSD results from our laboratory [17–19].

Assignments of hydrogen differential for the x and b ions were less unambiguous than the other ion series. In a few instances, multiply charged x ions displayed a loss of j hydrogens $(-j)$, whereas in other cases there was a $-(j - 1)$ hydrogen differential. In this initial study, we observed very few b ions and their appearance in conjunction with neutral loss complicated the spectra. As a result, a definitive determination on the number of hydrogens lost or gained for b ions could not be made in this study. The b-ion assignments reported here used a $-(j - 1)$ hydrogen differential, which was also our assignment in prior PSD studies [17–19]. However, recent work in our laboratory on simpler peptide systems suggests that b ions often have a $-(j + 1)$ hydrogen differential [37]. This differential, which would mean that b ions in the negative mode have two fewer hydrogens than their positive counterparts, has also been reported by Kulik and Heerma [11] for singly deprotonated ions. Efforts to resolve these issues as of assignment for multiply deprotonated b and x ions are currently underway in our laboratory. However, because neither ion is seen in abundance in the present work, this ambiguity does not affect the present results.

Hirudin (54–65) $[M - 3H]^{3-}$ and $[M - 2H]^{2-}$

Hirudin (54–65) is a fragment of the 65 residue protein, hirudin, which is the most prolific anticoagulant known. This highly anionic region of the protein is believed to be the active site for binding to thrombin, which hinders blood clotting [38]. Assuming that negative ions are typically deprotonated at the carboxylic acid group at the C-terminus and the side chains of aspartic acid (D) and glutamic acid (E) residues, hirudin

or lost hydrogens. In making these assignments, the experimentally observed assignments agreed within ± 0.02 m/z units of the theoretical value. For instance, fibrinopeptide B gives a theoretical a_2^{1-} ion of 141.066 m/z; this ion was found at 141.065 m/z in the FT-ICR

Table 1. Table of standard cleavages and neutral loss for $[M - 2H]^{2-}$ for hirudin (54–65)

Hir (54–65)	G	D^a	F	E	E	I	P	E	E	Y	L	Q
$n =$	1	2	3	4	5	6	7	8	9	10	11	12
b_n			w^{1-b}									
$y_{(13-n)}$					w^{1-}						w^{1-}	
$[a_n - 45]$			w^{1-}									
$[b_n - 36]$			w^{1-}									
$[b_n - 61]$			w^{1-}									
$[c_n - 35]$				w^{1-}				m^{1-}				
$[x_{(13-n)} - 33]$											w^{1-}	
$[x_{(13-n)} - 17]$											w^{1-}	
$[x_{(13-n)} - 36]$							w^{1-}					
$[y_{(13-n)} - 18]$			w^{1-}							m^{1-}	w^{1-}	
$[y_{(13-n)} - 34]$											w^{1-}	
$[y_{(13-n)} - 36]$										w^{1-}	s,^{c} $[M - 18]^{2-}$	
$[z_{(13-n)} - 36]$										w^{1-}	m, $[M - 36]^{2-}$	w, $[M - 54]^{2-}$

^{a}Potential deprotonation sites in boldface.
^{b}Intensities are w is weak (<30% of the base peak), m is medium (30%–60%), and s is strong (>60%). The superscript gives the charge on the fragment ion.
^{c}Neutral loss from parent ion.

Table 2. Table of internal ion fragments and neutral loss for [M − 2H]$^{2-}$ of hirudin (54–65)

Hir (54–65)	G	D^a	F	E	E	I	P	E	E	Y	L	Q
n =	1	2	3	4	5	6	7	8	9	10	11	12

Internal ion^c

$\overline{\text{w}^{1-},^{b}(\text{b}_1\text{y}_9)_2 - 61}$ (residues 2–3)

$\overline{\text{w}^{1-}, (\text{b}_4\text{y}_5)_3 - 57}$ (residues 5–8)
$\overline{\text{w}^{1-}, (\text{b}_4\text{y}_6)_2 - 18}$ (residues 5–7)
$\overline{\text{w}^{1-}, (\text{b}_4\text{y}_6)_2}$ (residues 5–7)

$\overline{\text{w}^{1-}, (\text{b}_8\text{y}_2)_2 - 18}$ (residues 9–10)
$\overline{\text{w}^{1-}, (\text{b}_7\text{y}_3)_2 - 36}$ (residues 8–10)
$\overline{\text{w}^{1-}, (\text{b}_8\text{y}_2)_2 - 36}$ (residues 9–10)
$\overline{\text{w}^{1-}, (\text{b}_7\text{y}_3)_2 - 18}$ (residues 8–10)

$\overline{\text{m}^{1-}, (\text{b}_2\text{y}_7)_3 - 18}$ (residues 3–6)
$\overline{\text{w}^{1-}, (\text{b}_1\text{y}_5)_6 - 44}$ (residues 2–7)
$\overline{\text{w}^{1-}, (\text{b}_3\text{y}_5)_4}$ (residues 4–7)
$\overline{\text{s}^{1-}, (\text{b}_5\text{y}_2)_5 - 36}$ (residues 6–10)

^{a}Potential deprotonation sites in boldface.
^{b}Intensities are w is weak (<30% of the base peak), m is medium (30%–60%), and s is strong (>60%). The superscript gives the charge on the fragment ion.
^{c}The internal ion is composed of the underlined residues.

(54–65) has six possible deprotonation sites. Our spectra show a maximum charge state of 3−, with 2− and 1− also being observed. This lack of full deprotonation might result from the close proximity of the glutamic acid residues (E^4 E^5 or E^8 E^9), which increases coulombic repulsion and thus may allow only one site of deprotonation between two adjacent residues.

For these initial studies, we investigated the dissociation of [M − nH]$^{n-}$, n = 3 and 2. Their SORI-CID spectra are shown in Figure 3. Tables 1–4 provide a detailed listing of the observed fragments for these two ions from SORI-CID mass spectra. Tables 1 and 3 list the standard cleavages, their relative intensities, and pertinent neutral losses for [M − 2H]$^{2-}$ and [M − 3H]$^{3-}$, respectively. Tables 2 and 4 list the internal fragment ions, their relative intensities, and neutral losses.

The spectra of the two parent ions are quite different, with more fragments being observed for [M − 3H]$^{3-}$. This mirrors the increased dissociation efficiency that is found as the charge increases for positive ions [39–42]. More highly charged ions have increased coulombic repulsion that enhances dissociation.

Table 3. Table of standard cleavages and neutral loss for [M − 3H]$^{3-}$ for hirudin (54–65)

Hir (54–65)	G	D^a	F	E	E	I	P	E	E	Y	L	Q
n =	1	2	3	4	5	6	7	8	9	10	11	12
a_n					w^{2-}							
b_n			w^{1-}	w^{1-}								
c_n		w$^{1-\,b}$										
$y_{(13-n)}$							w^{2-}				w^{1-}	
[b_n − 17]			w^{1-}									
[b_n − 36]			w^{1-}									
[b_n − 61]			w^{1-}									
[c_n − 17]			w^{1-}									
[c_n − 18]											w^{2-}	
[c_n − 34]			w^{1-}	w^{1-}								
[c_n − 35]			w^{1-}	w^{1-}		w^{1-}		w^{2-}, w^{1-}				
[c_n − 36]			w^{1-}								w^{2-}	
[c_n − 52]			w^{1-}					w^{1-}				
[$x_{(13-n)}$ − 17]											w^{1-}	
[$x_{(13-n)}$ − 35]							w^{1-}					
[$y_{(13-n)}$ − 17]											w^{1-}	
[$y_{(13-n)}$ − 18]				w^{2-}				w^{1-}	m^{2-}, w^{1-}		w^{1-}	
[$y_{(13-n)}$ − 34]											w^{1-}	
[$y_{(13-n)}$ − 36]		w^{3-}, w^{2-}							w^{1-}		w^{1-}	
[$y_{(13-n)}$ − 44]											w^{1-}	
[$y_{(13-n)}$ − 53]		w^{3-}									s,^{c} [M − 18]$^{3-}$	
[$y_{(13-n)}$ − 54]		w^{2-}									m, [M − 36]$^{3-}$	
											w, [M − 54]$^{3-}$	

^{a}Potential deprotonation sites are in boldface.
^{b}Intensities are w is weak (<30% of the base peak), m is medium (30%–60%), and s is strong (>60%). The superscript gives the charge on the fragment ion.
^{c}Neutral loss from parent ion.

Table 4. Table of internal ion fragments and neutral loss for $[M - 3H]^{3-}$ of hirudin (54–65)

Hir (54–65)	G	D^a	F	E	E	I	P	E	E	Y	L	Q
n =	1	2	3	4	5	6	7	8	9	10	11	12

Internal ion^b

- $w^{1-,c}$ $(b_1y_9)_2 - 61$ (residues 2–3)
- w^{1-}, $(b_4y_6)_2 - 17$ (residues 5–8)
- w^{1-}, $(b_8y_2)_2 - 18$ (residues 9–11)
- w^{1-}, $(b_4y_5)_3 - 57$ (residues 5–7)
- m^{1-}, $(b_4y_6)_2 - 18$ (residues 5–8)
- w^{1-}, $(b_4y_6)_2$ (residues 5–8)
- w^{1-}, $(b_8y_2)_2$ (residues 9–11)
- m^{1-}, $(b_4y_5)_3$ (residues 5–7)
- w^{-}, $(b_9y_1)_2$ (residues 10–11)
- w^{1-}, $(b_4y_5)_3 - 54$ (residues 5–7)
- m^{1-}, $(b_2y_7)_3 - 18$ (residues 3–7)
- w^{1-}, $(b_7y_1)_4$ (residues 8–11)
- w^{1-}, $(b_3y_5)_4$ (residues 4–7)

^a Potential deprotonation sites are in boldface.
^b The internal ion is composed of the underlined residues.
^c Intensities are w is weak (<30% of the base peak), m is medium (30%–60%), and s is strong (>60%). The superscript gives the charge on the fragment ion.

The data of Figure 3 reveal a predominance of c, x, and y series and internal ion fragments, which involve two cleavages of the peptide backbone. Very few a, b, and z series fragments are formed. The spectra show significant neutral loss; in particular, H_2O (18 Da) and NH_3 (17 Da). Sequential loss of H_2O occurs (e.g., $[y_8 - 36]^{1-}$) and the loss of combinations of neutrals is very common (e.g., $[x_6 - 35]^{1-}$, where $H_2O + NH_3 = 35$ Da, and $[b_3 - 61]^{1-}$, where $CO_2 + NH_3 = 61$ Da). As Tables 1 and 3 indicate, the parent ions for both charge states eliminate multiples of H_2O; for example, $[M - 18]^{n-}$, $[M - 36]^{n-}$, and $[M - 54]^{n-}$ (where $n = 2$ and 3). Loss of H_2O is indicative of glutamic or aspartic acid residues. Loss of NH_3 is associated with asparagine (N) residues [16, 43] and the present results suggest also with glutamine (Q). Other neutral eliminated include CO_2 (44 Da) and CH_3 (15 Da). Also, in Table 4, the internal ion $[(b_4y_5)_3 - 57]^{1-}$ is consistent with the presence of isoleucine (I^6). In singly deprotonated peptide ion CID, Bowie and co-workers have found that both isoleucine and leucine lose their butyl side chains (57 Da) [13–16, 23–25, 44]. In general, neutral loss is indicative of a specific amino acid residue and, in this manner, provides sequence information.

The fragments listed in Tables 1–4 suggest that the acidic residues (D, E, and the C-terminus) are likely sites of deprotonation [4, 45] and that these residues promote backbone fragmentation and side chain cleavages [23, 25]. Most fragments include at least one acidic residue and cleavage is often (but not always) adjacent to an acidic residue; for instance y_2^{1-} and y_8^{1-} in Table 1 or c_2^{1-} and y_6^{2-} in Table 3. The doubly charged y_6^{2-} ion, is most likely deprotonated at one of the glutamic residues (E^8, E^9) and the C-terminus. Cleavage can occur both N- and C-terminal to the site of deprotonation. For example, b_3^- involves cleavage N-terminal to E^4 and includes D^2. The internal ions frequently involve cleavages adjacent to acidic residues; for example, $(b_3y_4)_4^{1-}$, $[(b_7y_3)_2 - 2H_2O]^{1-}$ (Table 2) and $[(b_8y_2)_2 - H_2O]^{1-}$ and $(b_9y_1)_2^{1-}$ (Table 4). The y ions, which

incorporate the C-terminus, are dominated by loss of H_2O (18 Da). The c ions, which incorporate the N-terminus, lose a combination of H_2O and NH_3 (35 Da); for instance, fragments involving c_2, c_3, c_5, and c_7. These results are consistent with PSD data [46, 47], where

Figure 4. SORI-CID mass spectra of (a) $[M - 3H]^{3-}$ and (b) $[M - 4H]^{4-}$ for fibrinopeptide B.

Table 5. Table of standard cleavages and neutral loss for $[M - 3H]^{3-}$ of fibrinopeptide B

Fib. B	pE[a]	G	V	N	D[b]	N	E	E	G	F	F	S	A	R
n =	1	2	3	4	5	6	7	8	9	10	11	12	13	14
a_n		w^{1-c}			w^{1-}									
c_n	m^{1-}	w^{1-}	s^{1-}	w^{1-}										
$y_{(15-n)}$											w^{1-}	w^{1-}		w^{1-}
$[a_n - 35]$		w^{1-}												
$[a_n - 18]$		w^{1-}					w^{1-}							
$[a_n - 17]$		w^{1-}												
$[b_n - 34]$							w^{2-}							
$[b_n - 36]$								w^{1-}	w^{2-}					
$[b_n - 35]$									w^{1-}					
$[c_n - 34]$						w^{1-}								
$[c_n - 35]$		w^{1-}			w^{1-}									
$[c_n - 18]$		w^{1-}		m^{1-}	w^{1-}									
$[c_n - 17]$	m^{1-}					w^{1-}								
$[x_{(15-n)} - 36]$												w^{1-}		
$[x_{(15-n)} - 18]$												w^{1-}		
$[y_{(15-n)} - 54]$			w^{2-}											
$[y_{(15-n)} - 36]$			w^{2-}					w^{2-}						w^{1-}
$[y_{(15-n)} - 17]$					w^{2-}, w^{1-}									
$[y_{(15-n)} - 18]$											w^{1-}			
$[y_{(15-n)} - 42]$														w^{1-}
$[z_{(15-n)} - 33]$							w^{1-}						$w,^d\ [M - 34]^{3-}$	$w,\ [M - 44]^{3-}$

[a] pE symbolizes pyroglutamic acid.
[b] Potential deprotonation sites in boldface.
[c] Intensities are w is weak (<30% of the base peak), m is medium (30%–60%), and s is strong (>60%). The superscript gives the charge on the fragment ion.
[d] Neutral loss from parent ion.

Table 6. Table of internal ion fragments and neutral loss for $[M - 3H]^{3-}$ of fibrinopeptide B

Fib. B	pE[a]	G	V	N	D[b]	N	E	E	G	F	F	S	A	R
n =	1	2	3	4	5	6	7	8	9	10	11	12	13	14

Internal ion[c] — the internal ion is composed of the underlined residues:

- $w^{1-,d}$ $(b_3y_{10})_1$
- m^{-1}, $(b_1y_{11})_{2-}$
- w^{1-}, $(b_4y_8)_1 - 35$
- s^{1-}, $(b_7y_6)_1$
- w^{1-}, $(b_7y_5)_2$
- w^{1-}, $(b_3y_9)_2 - 17$
- w^{1-}, $(b_8y_4)_{2-}$
- w^{1-}, $(b_6y_6)_2$
- w^{1-}, $(b_4y_8)_2 - 18$
- w^{1-}, $(b_4y_8)_2 - 17$
- w^{1-}, $(b_9y_3)_2$
- w^{1-}, $(b_1y_{10})_3 - 17$
- w^{1-}, NDN $- 34$
- w^{1-}, $(b_6y_5)_3 - 18$
- w^{1-}, $(b_8y_3)_3$
- w^{1-}, $(b_6y_5)_3$
- w^{2-}, $(b_6y_2)_6$
- w^{2-}, $(b_6y_1)_7 - 30$
- m^{2-}, $(b_5y_2)_7 - 44$
- w^{1-}, $(b_2y_7)_5 - 34$
- w^{1-}, $(b_9y_1)_4 - 35$
- w^{1-}, $(b_8y_2)_4 - 17$
- w^{1-}, $(b_9y_1)_4 - 18$
- w^{1-}, $(b_7y_3)_4$
- w^{2-}, $(b_3y_2)_9 - 18$
- w^{1-}, $(b_4y_5)_5 - 34$
- w^{1-}, $(b_7y_2)_5 - 36$
- w^{1-}, $(b_7y_1)_6$

[a] pE symbolizes pyroglutamic acid.
[b] Potential deprotonation sites in boldface.
[c] The internal ion is composed of the underlined residues.
[d] Intensities are w is weak (<30% of the base peak), m is medium (30%–60%), and s is strong (>60%). The superscript gives the charge on the fragment ion.

Table 7. Table of standard cleavages and neutral loss for $[M - 4H]^{4-}$ for fibrinopeptide B

Fib. B	pE[a]	G	V	N	D[b]	N	E	E	G	F	F	S	A	R
n =	1	2	3	4	5	6	7	8	9	10	11	12	13	14
a_n		w^{1-c}												
c_n	w^{1-}	w^{1-}	m^{1-}	w^{2-}										
$x_{(15-n)}$		w^{4-}												
$y_{(15-n)}$						w^{3-}						w^{1-}		w^{1-}
$[a_n - 34]$		w^{1-}												
$[a_n - 35]$		w^{1-}										m,^{d}$[M - 62]^{4-}$		
$[a_n - 18]$		w^{1-}					w^{1-}					m,$[M - 34]^{4-}$		
$[b_n - 36]$									w^{1-}			s,$[M - 44]^{4-}$		
$[c_n - 18]$	w^{1-}		w^{1-}		w^{1-}				w^{2-}			w,$[M - 52]^{4-}$		
$[c_n - 17]$	w^{1-}				w^{1-}		w^{2-}		w^{2-}	w^{1-},w^{3-}				
$[c_n - 34]$						w^{1-}								
$[c_n - 35]$					w^{1-}									
$[x_{(15-n)} - 36]$														w^{1-}
$[y_{(15-n)} - 17]$								w^{1-}				w^{1-}		w^{1-}
$[y_{(15-n)} - 18]$													w^{1-}	
$[y_{(15-n)} - 16]$														w^{1-}
$[y_{(15-n)} - 45]$			w^{2-}											
$[y_{(15-n)} - 32]$												w^{1-}		
$[y_{(15-n)} - 36]$					w^{2-}							w^{1-}		w^{1-}
$[y_{(15-n)} - 42 - 18]$														w^{1-}
$[z_{(15-n)} - 33]$											w^{1-}			

^{a}pE symbolizes pyroglutamic acid.
^{b}Potential deprotonation sites in boldface.
^{c}Intensities are w is weak (<30% of the base peak), m is medium (30%–60%), and s is strong (>60%). The superscript gives the charge on the fragment ion.
^{d}Neutral loss from parent ion.

N-terminal fragments such as b and c ions were reported to lose NH_3 and, in some instances, H_2O. Furthermore, the loss of H_2O is observed from the aspartic acid and glutamic acid residues in the fragments (D^2, E^4, and E^5).

Using on-resonance CID, breakdown curves (not shown) were made of relative abundance for representative fragments versus laboratory frame collision energy, E_{lab}. The more highly charged $[M - 3H]^{3-}$ has greater coulomb energy than $[M - 2H]^{2-}$ and thus achieves significant dissociation at a lower threshold value of E_{lab} (~20 eV vs. 30 eV). For both parent ions, loss of H_2O is the lowest energy pathway. This is consistent with the fact that rearrangements to eliminate stable neutrals are lower energy processes than direct cleavages. At slightly higher energies cleavage of the peptide backbone occurs, while internal ions dominate at even higher energies. This is expected because internal ions involve cleavages at two bonds in the peptide backbone. In addition, loss of H_2O and other neutrals from the fragments becomes more prominent at higher collision energies. One particularly interesting process is the loss of CO_2 from y_2^{1-}; this high energy fragment is observed for $[M - 3H]^{3-}$, but not $[M - 2H]^{2-}$. Loss of CO_2 has been reported to originate from the C-terminal residue in dissociations of di- and tripeptide $[M - H]^-$ [13–15, 48].

Differences in fragmentation between the two charge states contribute to primary structure elucidation. For instance, the largest y ion observed for hirudin $[M - 2H]^{2-}$ is $[y_9 - H_2O]^{1-}$. The higher charge state produces $[y_{11} - 36]^{n-}$ (n = 2 and 3) as its largest y fragment. In addition, the internal ions can provide sequence information because the residues in the fragments overlap; for example, $(b_7y_1)_4^{1-}$, $(b_9y_1)_2^{1-}$, and $[(b_8y_2)_2 - H_2O]^{1-}$. The fragmentation patterns for the two charge states are therefore complementary to each other and provide a wealth of primary sequence information. In addition, SORI-CID produced fragments that were not observed by on-resonance CID; thus, SORI-CID yielded a greater amount of structural information. This is consistent with positive ion studies, where McLafferty and co-workers [41] found that SORI-CID provided more efficient dissociation than on-resonance CID for multiply charged positive ions.

Fibrinopeptide B [M − 4H]$^{4−}$ and [M − 3H]$^{3−}$

Fibrinopeptide B is a 14 residue peptide that is important in blood clotting. This peptide, along with fibrinopeptide A, is cleaved by thrombin from fibrinogen to initiate the formation of the blood clot. These anionic peptides are known to hinder fibrinogen aggregation by charge–charge repulsion [38]. Potential deprotonation sites in fibrinopeptide B are its three acidic residues and the C-terminus. Consistent with this, our spectra showed a maximum negative charge state of 4−.

Figure 4 gives the SORI-CID mass spectra for $[M - 3H]^{3-}$ and $[M - 4H]^{4-}$. Tables 5 and 7 list the standard cleavage fragments and neutral loss for $[M - 3H]^{3-}$ and $[M - 4H]^{4-}$, respectively. Tables 6 and 8 show the internal ions and their neutral eliminations. Similar to

Table 8.   Table of internal ion fragments and neutral loss for $[M - 4H]^{4-}$ of fibrinopeptide B

Fib. B	pE[a]	G	V	N	D[b]	N	E	E	G	F	F	S	A	R
n =	1	2	3	4	5	6	7	8	9	10	11	12	13	14

Internal ion[c]

$\overline{w^{1-}, (b_3y_9)_2 - 17}$ (cols V–N), $\overline{s^{-1}, (b_7y_6)_1}$ (col E9), $\overline{w^{1-}, (b_{10}y_3)_1}$ (cols F–F)

$\overline{w^{1-}, (b_3y_9)_2 - 35}$ (cols V–N)

$\overline{w^{1-}, (b_8y_4)_{2-}}$ (cols E–G)

$\overline{w^{1-}, (b_5y_7)_2 - 18}$ (cols N–E), $\overline{w^{1-}, (b_8y_4)_2}$ (cols E–G)

$\overline{w^{1-}, (b_6y_5)_3 - 18}$ (cols E–G)

$\overline{w^{1-}, (b_5y_7)_2 - 17}$ (cols N–E), $\overline{w^{1-}, (b_9y_2)_3 - 17}$ (cols G–F)

$\overline{w^{2-}, (b_3y_6)_5}$ (cols N–E)

$\overline{w^{3-}, (b_2y_4)_8}$ (cols N–E)

$\overline{w^{1-}, (b_3y_9)_2 - 34}$ (cols V–N)

$\overline{w^{3-}, (b_3y_3)_8}$ (cols E–S)

$\overline{w^{2-}, (b_5y_3)_6}$ (cols N–S)

$\overline{w^{2-}, (b_3y_2)_9 - 18}$ (cols N–E)

[a]pE symbolizes pyroglutamic acid.
[b]Potential deprotonation sites in boldface.
[c]The internal ion is composed of the underlined residues.
[d]Intensities are w is weak (<30% of the base peak), m is medium (30%–60%), and s is strong (>60%). The superscript gives the charge on the fragment ion.

the CID of hirudin, the fibrinopeptide B spectra are dominated by c and y cleavages and internal ions. Some b, a, and z ions also form. There is a distinct difference in dissociation patterns for the two parent ions. The spectrum of $[M - 4H]^{4-}$ is dominated by neutral loss (e.g., $[M - 44]^{4-}$, $[M - 34]^{4-}$, and $[M - 44 - 18]^{4-}$), whereas the spectrum of $[M - 3H]^{3-}$ does not show this neutral loss directly from the parent ion. In addition, other differences are found. For example, $[M - 4H]^{4-}$ produces $[z_4 - 33]^{1-}$ ($H_2O + CH_3 = 33$ Da), but no z ion is produced by $[M - 3H]^{3-}$. Niwa and co-workers [42] also observed differences in dissociation patterns for $[M + 2H]^{2-}$ and $[M + 3H]^{3+}$ for substance P and attributed this to the difference in coulomb energy of the two charge states.

Loss of neutrals from fragment ions is common for this peptide. For instance, $[c_n - 18]$, $n = 2, 3, 5$, and 9, are produced from $[M - 4H]^{4-}$. Furthermore, sequential loss of NH_3 is observed; for example, $[M - 34]^{4-}$ and $[M - 34]^{3-}$. Loss of NH_3 is reported to originate from asparagine (N) [16, 43]; it may also originate from glutamine (Q). This is consistent with the present results, where internal ions such as $[(b_3y_8)_3 - 34]^{1-}$ and $[(b_4y_8)_2 - 17]^{1-}$ lose NH_3. The loss of CH_3 (15 Da) is indicative of alanine (A) for singly charged negative peptide ions [13, 23, 25]. Our results also show that only fragments containing alanine give neutral loss of 15 Da; for example, $[z_4 - 33]^{1-}$ ($H_2O + CH_3 = 33$ Da) and $[y_3 - 32]^{1-}$ ($NH_3 + CH_3 = 32$ Da). Both parent ions, $[M - 3H]^{3-}$ and $[M - 4H]^{4-}$, produce fragments with loss of CO_2 (44 Da). As discussed in the previous section, this neutral loss is very common to negative ion dissociation and is thought to originate from the C-terminal residue [13–16, 24, 25, 44]. Loss of 30 Da, which is indicative of CH_2O elimination from serine [13], occurs for at least one internal ion fragment $[(b_6y_1)_7 -$
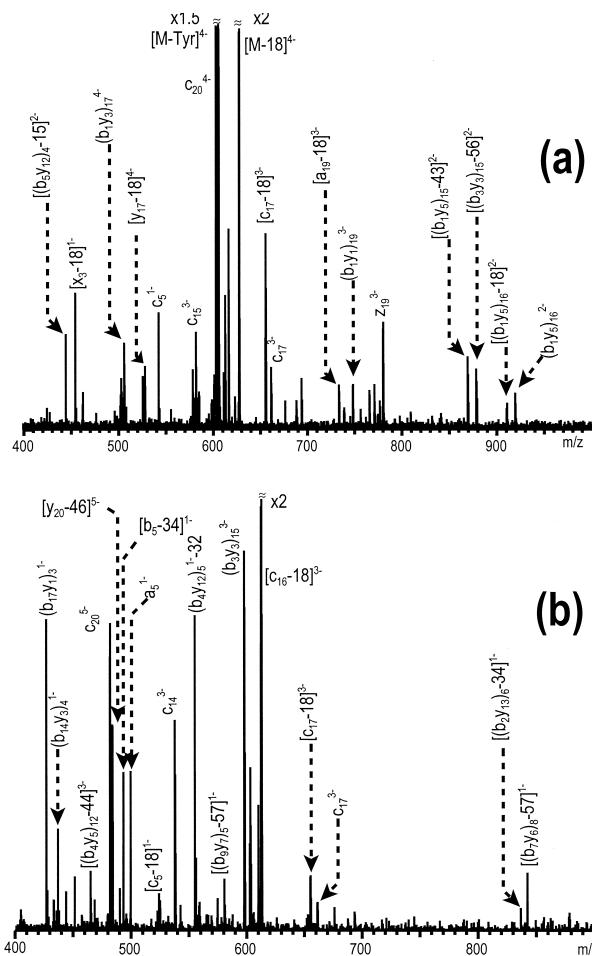
Figure 5. SORI-CID mass spectra of (a) $[M - 4H]^{4-}$ and (b) $[M - 5H]^{5-}$ for insulin chain A oxidized.

Table 9. Table of standard cleavages and neutral loss for $[M - 4H]^{4-}$ of insulin chain A oxidized

Insulin A	G	I	V	E[a]	Q	Cyx[b]	Cyx	A	S	V	Cyx	S	L	Y	Q	L	E	N	Y	Cyx	N
$n =$	1	2	3	4	5	6	7	8	9	10	11	12	13	14	15	16	17	18	19	20	21
a_n																			w^{3-}		
c_n								w^{2-c}							w^{3-}		w^{3-}		w^{4-}		
$z_{(22-n)}$		w^{3-}																			
$[a_n - 18]$																			w^{3-}		
$[b_n - 18]$																		w^{3-}			
$[c_n - 17]$																w^{3-}					
$[c_n - 18]$					w^{3-}																
$[c_n - 35]$																w^{3-}					
$[x_{(22-n)} - 18]$						w^{4-}													w^{-}		
$[x_{(22-n)} - 54]$				w^{3-}																	
$[y_{(22-n)} - 18]$					w^{4-}																
$[y_{(22-n)} - 44]$				w^{3-}																	m,[d] $[M - 18]^{4-}$
$[y_{(22-n)} - 61]$				w^{3-}																	w, $[M - 61]^{4-}$
$[z_{(22-n)} - 18]$				w^{3-}																	w, $[M - Tyr]^{4-}$

[a] Potential deprotonation sites are in boldface.
[b] Cyx symbolizes cysteic acid.
[c] Intensities are w is weak (<30% of the base peak), m is medium (30%–60%), and s is strong (>60%). The superscript gives the charge on the fragment ion.
[d] Neutral loss from parent ion.

30]$^{1-}$. Loss of 42 Da, HN=C=NH, is indicative of arginine [23, 25] and is only observed for fragments containing this residue; for instance, $[y_1 - 42 - 18]^{1-}$.

Using on-resonance CID data, breakdown curves were made of product formation versus collision energy for fibrinopeptide B ions. They exhibit the same trends that were found for hirudin (54–65). That is, neutral loss from the parent ion is the lowest energy process; for example, the fragment $[M - 4H - NH_3]^{4-}$ reaches a maximum at ~50 eV but then quickly disappears to less than 5% relative abundance. As the collision energy increases, first standard peptide cleavages occur, followed by internal ion formation, and then neutral loss from these fragments.

The $[M - 4H]^{4-}$ and $[M - 3H]^{3-}$ CID data provide complementary information. Neither parent ion cleavages at every residue, but between the two spectra, cleavage at every residue occurs (albeit often with neutral loss). From the y and c ions in Tables 5 and 7, there is cleavage at every residue; for instance, c_n^{d-}, $n = 1$–4 and then a combination of $[y_n - 17]^{1-}$ and $[y_n - 18]^{d-}$ ions. Furthermore, the prevalent internal ions, for example $(b_6y_2)_6^{1-}$ and $[(b_6y_1)_7 - 30)]^{1-}$, can provide sequence information. In this manner, complete primary structural elucidation is obtained from this single, underivatized peptide by employing low-energy dissociation techniques.

Insulin Chain A (Oxidized) $[M - 4H]^{4-}$ and $[M - 5H]^{5-}$

Insulin chain A (oxidized) is a 21 residue peptide that is part of the insulin hormone, which is pivotal in glucose metabolism [38]. The peptide has six acidic residues, including four highly acidic sulfated cystine residues (i.e., cysteic acid residues) and the C-terminus as potential deprotonation sites. A maximum charge state of

Table 10. Table of internal ion fragments and neutral loss for $[M - 4H]^{4-}$ of insulin chain A oxidized

Insulin A	G	I	V	E[a]	Q	Cyx[b]	Cyx	A	S	V	Cyx	S	L	Y	Q	L	E	N	Y	Cyx	N
$n =$	1	2	3	4	5	6	7	8	9	10	11	12	13	14	15	16	17	18	19	20	21

Internal ion[c]

- w^{4-}, $(b_1y_3)_{17}$
- w^{2-}, $(b_1y_5)_{15} - 34$
- w^{4-}, $(b_1y_1)_{19}$
- w^{3-}, $(b_1y_4)_{17}$
- w^{3-}, $(b_1y_2)_{18} - 18$
- w^{3-}, $(b_1y_2)_{18}$
- w^{3-}, $(b_1y_1)_{19}$

[a] Potential deprotonation sites in boldface.
[b] Cyx symbolizes cysteic acid.
[c] Intensities are w is weak (<30% of the base peak), m is medium (30%–60%), and s is strong (>60%). The superscript gives the charge on the fragment ion.
[d] The internal ion is composed of the underlined residues.

Table 11. Table of standard cleavages and neutral loss for $[M - 5H]^{5-}$ of insulin chain A oxidized

Insulin A	G	I	V	E[a]	Q	Cyx[b]	Cyx	A	S	V	Cyx	S	L	Y	Q	L	E	N	Y	Cyx	N
$n =$	1	2	3	4	5	6	7	8	9	10	11	12	13	14	15	16	17	18	19	20	21
a_n						w^{1-c}										w^{3-}					
c_n						w^{1-}							w^{3-}			w^{3-}			w^{5-}, w^{4-}		
$y_{(22-n)}$																					
$[b_n - 34]$						w^{1-}												w^{1-}	w^{1-}		
$[c_n - 18]$						w^{1-}										s^{3-}		w^{3-}	w^{3-}		
$[x_{(22-n)} - 88]$				w^{5-}																	
$[y_{(22-n)} - 18]$																			m^{1-}		
$[y_{(22-n)} - 44]$				w^{5-}						w^{3-}											

[a] Potential deprotonation sites are in boldface.
[b] Cyx symbolizes cysteic acid.
[c] Intensities are w is weak (<30% of the base peak), m is medium (30%–60%), and s is strong (>60%). The superscript gives the charge on the fragment ion.

$[M - 7H]^{7-}$ has been previously reported [4, 45]. Under our ESI/FT-ICR conditions, the major parent ions were $[M - nH]^{n-}$, n = 2–6.

The most intense ions, $[M - 4H]^{4-}$ and $[M - 5H]^{5-}$, were chosen for CID studies. Figure 5 gives their SORI-CID spectra. Tables 9 and 11 list the standard peptide cleavages, while Tables 10 and 12 list the internal fragment ions. As was the case with the other two peptide systems, the dissociation products are primarily c, y, and internal ions, with significant neutral loss.

Relative to the other two peptides studied, insulin A shows less neutral loss from its parent ions and less abundant loss of multiple neutrals in its fragment ions. The reason for this difference is not clear. It is possible that H_2O elimination involves adjacent aspartic acids and glutamic acid residues, which do not occur in this peptide. Furthermore, insulin A is significantly larger than the other two peptides; there may be conformational factors that prohibit the rearrangements that are necessary for neutral eliminations. Also, insulin A $[M - 5H]^{5-}$ did not give any neutral elimination directly from the parent ion under SORI-CID conditions, al-though $[M - 4H]^{4-}$ eliminates H_2O and a tyrosine side chain (106 Da). (Loss of 106 Da from tyrosine has previously been reported in the negative ion mode [15, 23].) In contrast, for the two other peptides, the higher charge state parent ions gave more neutral loss than the lower charge state ions.

For $[M - 5H]^{5-}$, a number of fragments retain the charge of the parent ion; for instance, c_{20}^{5-} in Table 11 and c_{20}^{4-} in Table 9. These fragments suggest that the acidic residues, E^4, Cyx^6, Cyx^7, Cyx^{11}, E^{17}, and Cyx^{20} are likely sites of deprotonation. In fact, for c_{20}^{5-}, it is probable that either Cyx^6 or Cyx^7 is deprotonated, along with four other deprotonation sites to produce the c_{20}^{5-} ion. In addition, internal ion fragments are formed with only the N- and C-terminus residues cleaved. These fragments were also multiply charged, for example, $(b_1y_9)_{19}^{4-}$ and $(b_1y_1)_{19}^{3-}$ (see Table 10). They further support the concept that the acidic residues are sites of deprotonation. For internal ions, at least one of the backbone cleavages occurs adjacent to an acidic group (Cyx^{20} and N^{21}). This is consistent with acidic residues promoting fragmentation both C- and N-terminal to the deprotonation site (as was observed for the

Table 12. Table of internal ion fragments and neutral loss for $[M - 5H]^{5-}$ of insulin chain A oxidized

Insulin A	G	I	V	E[a]	Q	Cyx[b]	Cyx	A	S	V	Cyx	S	L	Y	Q	L	E	N	Y	Cyx	N
$n =$	1	2	3	4	5	6	7	8	9	10	11	12	13	14	15	16	17	18	19	20	21

Internal ion[c] (the internal ion is composed of the underlined residues)

- m^{1-}, $(b_4y_{12})_5 - 32$ (spans residues 5–12)
- w^{1-},[d] $(b_{14}y_3)_4$ (spans residues 17–19)
- w^{1-}, $(b_{11}y_6)_4$ (spans residues 11–16)
- w^{1-}, $(b_1y_{16})_4 - 17$ (spans residues 2–16)
- m^{1-}, $(b_9y_7)_5 - 57$ (spans residues 10–15)
- w^{1-}, $(b_1y_{16})_4$ (spans residues 2–16)
- w^{1-}, $(b_{14}y_2)_5 - 36$ (spans residues 16–20)
- m^{3-}, $(b_3y_3)_{15}$ (spans residues 4–18)
- w^{2-}, $(b_3y_3)_{15} - 57$ (spans residues 4–18)
- w^{1-}, $(b_2y_{13})_6 - 34$ (spans residues 3–8)
- w^{3-}, $(b_4y_5)_{12} - 44$ (spans residues 5–16)

[a] Potential deprotonation are sites in boldface.
[b] Cyx symbolizes cysteic acid.
[c] The internal ion is composed of the underlined residues.
[d] Intensities are w is weak (<30% of the base peak), m is medium (30%–60%), and s is strong (>60%). The superscript gives the charge on the fragment ion.

other two peptides). In a previous report on the dissociation of $[M - 4H]^{4-}$ for insulin chain A oxidized, Loo et al. [4] found prevalent b and y ions and significant loss of SO_3 (80 Da). In the present study, no such neutral loss is seen for either multiply charged parent ion. In addition, Loo et al. [4] did not observe the significant c ions or internal ions that are found in the present study. It is probable that many of these differences lie in data interpretation. In the triple quadrupole study [4], peaks were relatively broad, with low resolution; our FT-ICR data gave sharper peaks at much higher resolutions, which facilitated assignments of ion mass and formula. In particular, the higher resolution of the FT-ICR allowed us to unambiguously determine the charge states of the fragment ions by using the mass-to-charge spacings of the carbon-13 isotopic peaks [49].

Sequence information is more difficult to obtain from the oxidized insulin A CID spectra than it is from the spectra of the two smaller peptides. For oxidized insulin A, primary structural information must be garnered from the internal fragments because no series of ions give cleavage at every residue. This relative lack of fragmentation suggests that the highly acidic cysteic acid residues are localizing the charge and limiting fragmentation, in analogy to what has been reported by Summerfield and Gaskell [29] for three small peptides containing cysteic acid. Also, in the positive mode, highly basic arginine residues can sequester the charge and limit dissociation [50–52].

Conclusions

The dissociation patterns for multiply charged negative ions of three commercially available peptides were investigated using low-energy CID in a FT-ICR mass spectrometer. These compounds are highly acidic and did not produce sufficient positive ions for study by CID. The negative mode spectra indicated that the likely deprotonation sites are acidic residues (aspartic, glutamic, and cysteic acids) and the C-terminus. The spectra are rife with c, y, and internal ions, although some a, b, x, and z ions form. Many fragment ions were produced from cleavage adjacent to acidic residues, both N- and C-terminal to the acidic site. In addition, neutral loss (e.g., NH_3, CH_3, H_2O, and CO_2) occurs from the parent ions and the fragment ions. Neutral eliminations were often indicative of specific amino acid residues. The fragmentation patterns from several charge states of the parent ions, when combined, provide significant primary sequence information. The present results suggest that negative peptide ion dissociation of highly acidic peptides provides useful structural information in cases where positive ion dissociation does not provide sufficient ion signal.

References

1. Wong, S. F.; Meng, C. K.; Fenn, J. B. *J. Phys. Chem.* **1988,** *92,* 546–550.
2. Whitehouse, C. M.; Dreyer, R. N.; Yamshita, M.; Fenn, J. B. *Anal. Chem.* **1985,** *57,* 675–679.
3. Smith, R. D.; Loo, J. A.; Edmonds, C. G.; Barinaga, C. J.; Udseth, H. R. *Anal. Chem.* **1990,** *62,* 882–899.
4. Loo, J. A.; Loo, R. R. O.; Light, K. J.; Edmonds, C. G.; Smith, R. D. *Anal. Chem.* **1992,** *64,* 81–88.
5. Papayannopoulos, I. A. *Mass Spectrom. Rev.* **1995,** *14,* 49–73.
6. Vekey, K.; Somogyi, A.; Wysocki, V. H. *Rapid Commun. Mass Spectrom.* **1996,** *10,* 911–918.
7. Barinaga, C. J.; Edmonds, C. G.; Udseth, H. R.; Smith, R. D. *Rapid Commun. Mass Spectrom.* **1989,** *3,* 160–164.
8. Biemann, K.; Martin, S. A. *Mass Spectrom. Rev.* **1987,** *6,* 1–76.
9. Biemann, K. *Biomed. Environ. Mass Spectrom.* **1988,** *16,* 99–111.
10. Biemann, K. *Anal. Chem.* **1986,** *58,* 1288A–1300A.
11. Kulik, W.; Heerma, W. *Biomed. Environ. Mass Spectrom.* **1989,** *18,* 910–917.
12. Kulik, W.; Heerma, W. *Biol. Mass Spectrom.* **1991,** *20,* 553–558.
13. Waugh, R. J.; Eckersley, M.; Bowie, J. H.; Hayes, R. N. *Int. J. Mass Spectrom. Ion Processes* **1990,** *98,* 134–145.
14. Eckersley, M.; Bowie, J. H.; Hayes, R. N. *Int. J. Mass Spectrom. Ion Processes* **1989,** *93,* 199–213.
15. Waugh, R. J.; Bowie, J. H.; Hayes, R. N. *Int. J. Mass Spectrom. Ion Processes* **1991,** *107,* 333–347.
16. Bradford, A. M.; Waugh, R. J.; Bowie, J. H. *Rapid Commun. Mass Spectrom.* **1995,** *9,* 677–685.
17. Jai-nhuknan, J.; Cassady, C. J. *Anal. Chem.* **1998,** *70,* 5122–5128.
18. Jai-nhuknan, J.; Cassady, C. J. *J. Am. Soc. Mass Spectrom.* **1998,** *9,* 540–544.
19. Jai-nhuknan, J.; Cassady, C. *Rapid Commun. Mass Spectrom.* **1996,** *10,* 1678–1682.
20. Spengler, B.; Kersch, D.; Kaufmann, R.; Jaeger, E. *Rapid Commun. Mass Spectrom.* **1992,** *6,* 105–108.
21. Spengler, B.; Kirsch, D.; Kaufmann, R. *J. Phys. Chem.* **1992,** *96,* 9678–9684.
22. Spengler, B.; Kirsch, D.; Kaufmann, R. *Rapid Commun. Mass Spectrom.* **1991,** *5,* 198–202.
23. Steinbrenner, S. T.; Bowie, J. H. *Rapid Commun. Mass Spectrom.* **1997,** *11,* 253–258.
24. Raftery, M. J.; Bowie, J. H. *Int. J. Mass Spectrom. Ion Processes* **1988,** *85,* 167–186.
25. Waugh, R. J.; Bowie, J. H. *Rapid Commun. Mass Spectrom.* **1994,** *8,* 169–173.
26. Marzluff, E. M.; Campbell, S.; Rodgers, M. T.; Beauchamp, J. L. *J. Am. Chem. Soc.* **1994,** *116,* 7787–7796.
27. Gibson, B. W.; Cohen, P. In *Methods in Enzymology*; McCloskey, J. A., Ed.; Academic: San Diego, CA, 1990; pp 480–501.
28. Gibson, B. W. In *Biological Mass Spectrometry*; Burlingame, A. L.; McCloskey, J. A., Eds.; Elsevier: Amsterdam, 1990; pp 315–336.
29. Summerfield, S. G.; Gaskell, S. J. *Int. J. Mass Spectrom. Ion Processes* **1997,** *165/166,* 509–521.
30. Dale, V. C. M.; Speir, J. P.; Kruppa, G. H.; Stacey, C. C.; Mann, M.; Wilm, M. *Biochem. Mass Spectrom.* **1996,** *24,* 943–947.
31. Cassady, C. J.; Wronka, J.; Kruppa, G. H.; Laukien, F. H. *Rapid Commun. Mass Spectrom.* **1994,** *8,* 394–400.
32. Bruins, A. P.; Covey, T. R.; Henion, J. D. *Anal. Chem.* **1987,** *59,* 2642–2646.

33. Covey, T. R.; Bonner, R. F.; Shushan, B. I.; Henion, J. *Rapid Commun. Mass Spectrom.* **1988,** *2*, 249–256.
34. Gauthier, J. W.; Trautman, T. R.; Jacobson, D. B. *Anal. Chim. Acta* **1991,** *246*, 211–225.
35. Cody, R. B.; Burnier, R. C.; Freiser, B. S. *Anal. Chem.* **1982,** *54*, 96–101.
36. Roepstorff, P.; Fohlman, J. *Biomed. Mass Spectrom.* **1984,** *11*, 601.
37. Cassady, C. J.; Yalcin, T., unpublished results.
38. Voet, D.; Voet, J. G. *Biochemistry, 2nd ed*.; Wiley: New York, 1995.
39. Loo, J. A.; Edmonds, C. G.; Smith, R. D. *Anal. Chem.* **1993,** *65*, 425–438.
40. Williams, E. R. *J. Mass Spectrom.* **1996,** *31*, 831–842.
41. Senko, M. W.; Speir, J. P.; McLafferty, F. W. *Anal. Chem.* **1994,** *66*, 2801–2808.
42. Ishikawa, K.; Nishimura, T.; Koga, Y.; Niwa, Y. *Rapid Commun. Mass Spectrom.* **1994,** *8*, 933–938.
43. Waugh, R. J.; Bowie, J. H.; Gross, M. L. *Aust. J. Chem.* **1993,** *46*, 693–702.
44. Steinborner, S. T.; Bowie, J. H. *Rapid Commun. Mass Spectrom.* **1990,** *10*, 1243–1247.
45. Bruce, J. E.; Cheng, X.; Bakhtiar, R.; Wu, Q.; Hofstadler, S. A.; Anderson, G. A.; Smith, R. D. *J. Am. Chem. Soc.* **1994,** *116*, 7839–7847.
46. McCloskey, J. A. In *Methods in Enzymology*; McCloskey, J., Ed.; Academic: San Diego, CA, 1990; pp 330–339.
47. Brauman, J. L. *Kinetics of Ion–Molecule Reactions, 1st ed*.; Plenum: New York, 1979.
48. Waugh, R. J.; Bowie, J. H.; Gross, M. L.; Vollmer, D. *Int. J. Mass Spectrom. Ion Processes* **1994,** *133*, 165–174.
49. Henry, K. D.; Quinn, J. P.; McLafferty, F. W. *J. Am. Chem. Soc.* **1991,** *113*, 5447–5449.
50. Vachet, R. W.; Asam, M. R.; Glish, G. L. *J. Am. Chem. Soc.* **1996,** *118*, 6252–6256.
51. Johnson, R. S.; Martin, S. A.; Biemann, K. *Int. J. Mass Spectrom. Ion Processes* **1988,** *86*, 137–154.
52. Tang, X.; Thibault, P.; Boyd, R. K. *Anal. Chem.* **1993,** *65*, 2824–2834.